Supporting Information for "Numerical modeling of iceberg capsize responsible for glacial earthquakes"

Amandine Sergeant[1,2,3], Vladislav A. Yastrebov[4], Anne Mangeney[1,2,5],

Olivier Castelnau[6], Jean-Paul Montagner[1,2], Eléonore Stutzmann[1]

Corresponding author: Amandine Sergeant, Versuchsanstalt für Wasserbau, Hydrologie und Glaziologie, ETH Zürich, Hönggerbergring 26, 8093 Zürich, Switzerland. (sergeant@vaw.baug.ethz.ch)

[1]Institut de Physique du Globe de Paris, CNRS UMR 7154, Université Paris Diderot-Paris 7, Paris, France

[2]Université Paris Diderot, Paris, France

[3]Now at Versuchsanstalt für Wasserbau, Hydrologie und Glaziologie (VAW), ETH Zürich, CH-8092 Zürich, Switzerland (sergeant@vaw.baug.ethz.ch)

[4]MINES ParisTech, PSL Research University, Centre des Matériaux, CNRS UMR 7633, Evry, France

[5]ANGE team, INRIA, Laboratoire Jacques-Louis Lions, Paris, France

[6]Processes and Engineering in Mechanics and Materials, CNRS UMR 8006, ENSAM, CNAM, Paris, France

Contents of this file

1. Text S1: Discussion related to figure S2 and influence of initial buoyant conditions on the capsize force.

2. Figure S1: Drag effect on force magnitudes with the iceberg aspect ratio.

3. Figure S2: Effects of non-buyant initial conditions on the force spectral amplitudes at specific frequencies.

4. Movie S1: Animation of the bottom-out capsize of an iceberg of aspect ratio $\epsilon = 0.2$ and height $H = 800$ m, and associated contact force $F_c(t)$.

5. Movie S2: Animation of the topout capsize of an iceberg of aspect ratio $\epsilon = 0.2$ and height $H = 800$ m, and associated contact force $F_c(t)$.

6. Movie S3: Animation of the bottom-out capsize of a subaerial iceberg of aspect ratio $\epsilon = 0.1$ and height $H = 800$ m, and associated contact force $F_c(t)$.

Text S1.

As shown in the main body of the paper, initial buoyant conditions of the iceberg impacts the contact force. When they capsize, subaerial icebergs ($\Delta < 0$) generate a force whose spectral amplitudes are amplified at specific frequencies, noted f_{plus}. Similarly, submarine icebergs ($\Delta > 0$) generate a force with strong energy gap at frequencies f_{gap}. Figure S2 shows the evolution of these frequencies with the aspect ratio ϵ of the iceberg. The results presented here are for BO icebergs with $H = 800$ m. The same tendencies are observed for other iceberg heights but with slight shifts of f_{plus} and f_{gap} values toward higher or lower frequencies. For 600 m-height icebergs, they vary within the range 0.018-0.3 Hz. For 1000 m-height icebergs, they vary between 0.012 and 0.02 Hz. We also evaluate associated perturbations ΔA of the force spectral amplitudes at corresponding frequencies $f_0 = f_{\text{plus}}$ or $f_0 = f_{\text{gap}}$, with respect to the spectral amplitude of the neutral force as:

$$\Delta A(f_0) = \frac{A_{\Delta z}(f_0) - A_{z_w}(f_0)}{A_{z_w}(f_0)} \tag{1}$$

A represents the spectral amplitude, $A_{\Delta z}$ is for Δz-pertubated icebergs, A_{z_w} is for neutrally buoyant icebergs. Positive $\Delta A(f_{\text{plus}})$ are associated with subaerial icebergs. Negative $\Delta A(f_{\text{gap}})$ associated with submarine icebergs.

Figure S1. (a) Force magnitudes A (kg.m) computed by integrating the contact force twice with respect to time, for no drag (filled circles) and drag (open circles). The results are for bottom-out icebergs of unit length L. (b) Evolution of the ratio of the force magnitudes (drag/no drag) with ϵ. This shows that pressure drag greatly changes the capsize dynamics especially for thin icebergs.

Figure S2. Variation of the frequency (b) f_{plus} for the secondary force spectral peaks associated with subaerial icebergs, and (c) f_{gap} for the force energy gaps associated with submarine icebergs, with ϵ. Variation of the perturbations of force spectral amplitudes ΔA induced by $\Delta z \neq 0$ and measured at frequencies (d) f_{plus} and (e) f_{gap}, with aspect ratio. Results are for bottom-out icebergs with $H = 800$ m.

Movie S1. Animation of the bottom-out capsize of an iceberg of aspect ratio $\epsilon = 0.2$ and height $H = 800$ m, and associated force $F_c(t)$. The iceberg is initially at its hydrostatic equilibrium. The color scale represents horizontal stress σ_{xx}. Gray shaded area represents water.

Movie S2. Animation of the top-out capsize of an iceberg of aspect ratio $\epsilon = 0.2$ and height $H = 800$ m, and associated force F_c. The iceberg is initially at its hydrostatic equilibrium. The color scale represents horizontal stress σ_{xx}. Gray shaded area represents water.

Movie S3. Animation of the bottom-out capsize of a subaerial iceberg of aspect ratio $\epsilon = 0.1$ and height $H = 800$ m which experiences a water level $z_0 = z_w - 10$ m. Associated contact force F_c is plotted on the bottom panel. The color scale represents horizontal stress σ_{xx} of solid bodies. Gray shaded area represents water.

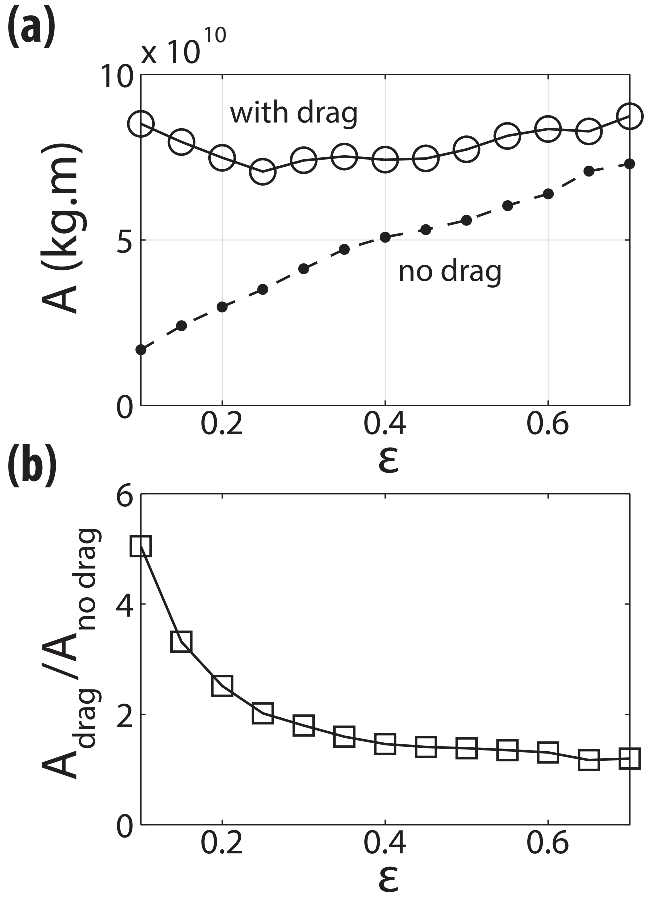

Figure S1. (a) Force magnitudes A (kg.m) computed by integrating the contact force twice with respect to time, for no drag (filled circles) and drag (open circles). The results are for bottom-out icebergs of unit length L. (b) Evolution of the ratio of the force magnitudes (drag/no drag) with ϵ. This shows that pressure drag greatly changes the capsize dynamics especially for thin icebergs.

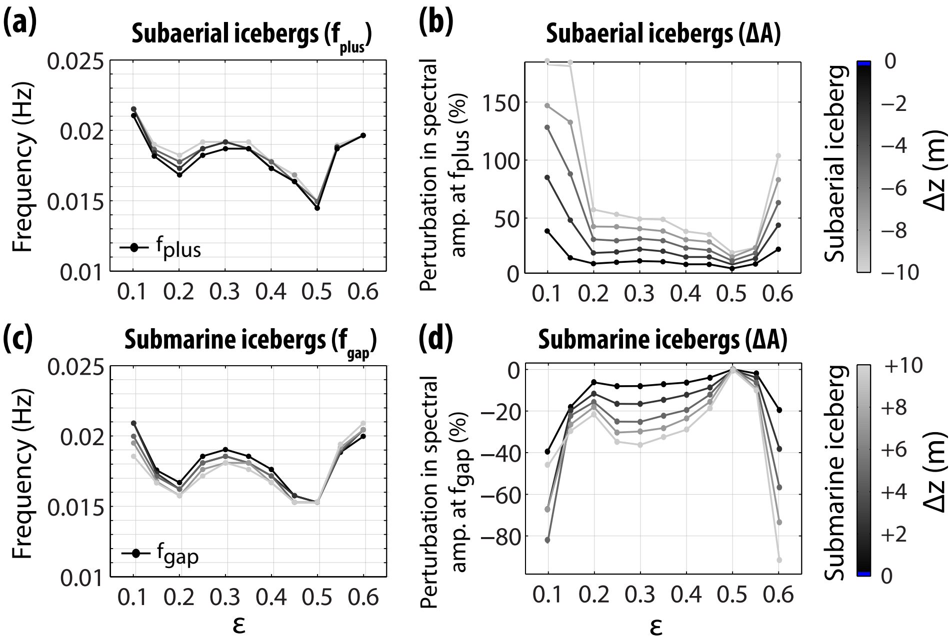

Figure S2. Variation of the frequency (b) f_{plus} for the secondary force spectral peaks associated with subaerial icebergs, and (c) f_{gap} for the force energy gaps associated with submarine icebergs, with ϵ. Variation of the perturbations of force spectral amplitudes ΔA induced by $\Delta z \neq 0$ and measured at frequencies (d) f_{plus} and (e) f_{gap}, with aspect ratio. Results are for bottom-out icebergs with $H = 800$ m.